BJ www.biochemj.org

BJ Metabolism

Biochem. J. (2011) **434**, 49–60 (Printed in Great Britain) doi:10.1042/BJ20101721

LKB1 is required for hepatic bile acid transport and canalicular membrane integrity in mice

Angela WOODS*[1], Amanda J. HESLEGRAVE*, Phillip J. MUCKETT*, Adam P. LEVENE†, Melanie CLEMENTS‡, Margaret MOBBERLEY§, Timothy A. RYDER§, Shadi ABU-HAYYEH‖, Catherine WILLIAMSON‖, Robert D. GOLDIN†, Alan ASHWORTH¶, Dominic J. WITHERS** and David CARLING*[1]

*Cellular Stress Group, MRC Clinical Sciences Centre, Imperial College, London, W12 0NN, U.K., †Department of Histopathology, Imperial College, London W2 IPG, U.K., ‡MRC Clinical Sciences Centre, Molecular Embryology, Imperial College, London W12 0NN, U.K., §Department of Histopathology, Charing Cross Hospital, London SW7 2AZ, U.K., ‖Institute of Reproductive and Developmental Biology, Imperial College, London W12 0NN, U.K., ¶The Breakthrough Breast Cancer Research Centre, The Institute of Cancer Research, London SW7 3RP, U.K., and **Metabolic Signalling Group, MRC Clinical Sciences Centre, Imperial College, London W12 0NN, U.K.

LKB1 is a 'master' protein kinase implicated in the regulation of metabolism, cell proliferation, cell polarity and tumorigenesis. However, the long-term role of LKB1 in hepatic function is unknown. In the present study, it is shown that hepatic LKB1 plays a key role in liver cellular architecture and metabolism. We report that liver-specific deletion of LKB1 in mice leads to defective canaliculi and bile duct formation, causing impaired bile acid clearance and subsequent accumulation of bile acids in serum and liver. Concomitant with this, it was found that the majority of BSEP (bile salt export pump) was retained in intracellular pools rather than localized to the canalicular membrane in hepatocytes from LLKB1KO (liver-specific *Lkb1*-knockout) mice. Together, these changes resulted in toxic accumulation of bile salts, reduced liver function and failure to thrive. Additionally, circulating LDL (low-density lipoprotein)-cholesterol and non-esterified cholesterol levels were increased in LLKB1KO mice with an associated alteration in red blood cell morphology and development of hyperbilirubinaemia. These results indicate that LKB1 plays a critical role in bile acid homoeostasis and that lack of LKB1 in the liver results in cholestasis. These findings indicate a novel key role for LKB1 in the development of hepatic morphology and membrane targeting of canalicular proteins.

Key words: AMP-activated protein kinase (AMPK), ATP-binding-cassette subfamily B, member 11 (ABCB11), bile salt export pump (BSEP), cholestasis, hyperbilirubinaemia, polarity.

INTRODUCTION

LKB1 encodes an evolutionarily conserved serine/threonine protein kinase that was originally identified as a tumour suppressor, as inactivating mutations in LKB1 in humans cause Peutz–Jeghers syndrome [1,2]. More recently, LKB1 has been shown to act upstream of AMPK (AMP-activated protein kinase) [3–5] and 12 AMPK-related kinases [6]. LKB1 phosphorylates a conserved threonine residue within the T-loop of these kinases, which is essential for their activation [7]. Activation of AMPK by LKB1 under conditions of energy depletion results in the down-regulation of energy-consuming pathways and the up-regulation of ATP-producing pathways. Much less is understood regarding the roles of the AMPK-related kinases, although there is evidence to suggest that the MARK [MAP (microtubule-associated protein)-regulating kinase/microtubule affinity-regulating kinase] [8] and BRSK (brain-specific kinase) [9,10] subfamilies play roles in determining cell polarity. Information concerning the physiological function of the remaining AMPK-related kinases is extremely limited [11].

Germline deletion of LKB1 leads to an embryonic-lethal phenotype with mice dying from a variety of vascular and placental defects, demonstrating a key developmental role [12]. Tissue-specific deletion of LKB1 has been investigated in several mouse models [13–15] with phenotypes affecting various aspects of cell morphology and organ dysfunction. Taken together these findings suggest that LKB1 plays a key role in integrating cell and tissue morphology with metabolic function.

The liver has many metabolic functions including bile production together with key regulatory roles in glucose, lipid and xenobiotic metabolism. Bile is the main vehicle by which the body disposes of excess cholesterol by conversion into bile acids and the route used for the excretion of waste products such as bilirubin, a breakdown product of haem. Because high levels of bile acids can cause tissue damage due to their strong detergent properties, their concentrations are tightly regulated by transcriptional control of many genes in a complex feedback mechanism involving bile acid activation of FXR (farnesoid X receptor) (reviewed in [16]). Following their synthesis in the liver, bile acids are secreted into the bile, stored in the gall bladder and released postprandially into the small intestine, where they play a critical role in the absorption of fat and fat-soluble nutrients. The majority of the bile acids are then returned to the liver via the portal circulation through ASBT (apical sodium-dependent bile acid transporter) in the epithelial cells of the small intestine. Completion of the enterohepatic circulation occurs when the bile acids are returned to the liver mainly by transport via NTCP (sodium–taurochloate co-transporting protein). A major feature

Abbreviations used: ABC, ATP-binding-cassette; ABCB11, ABC subfamily B, member 11; ABCG5/8, ABC subfamily G, member 5/8; ALP, alkaline phosphatase; ALT, alanine transaminase; AMPK, AMP-activated protein kinase; AST, aspartate transaminase; BSEP, bile salt export pump; CYP7A1, cytochrome P450, family 7, subfamily A, polypeptide 1; *Cypb*, cyclophilin b; FGF, fibroblast growth factor; FXR, farnesoid X receptor; HDL, high-density lipoprotein; LDL, low-density lipoprotein; LLKB1KO, liver-specific *Lkb1*-knockout; LP-X, lipoprotein-X; MRP, multi-drug resistance protein; NTCP, sodium–taurochloate co-transporting protein; OATP1, organic anion transporting polypeptide 1; qRT-PCR, quantitative real-time PCR; SHP, small heterodimer partner; T_3, tri-iodothyronine.

[1] Correspondence may be addressed to either of these authors (email angela.woods@imperial.ac.uk or david.carling@imperial.ac.uk).

of hepatocytes is their marked anatomical polarity, which plays an essential role in their function. For example, the polar nature of hepatocytes allows the efficient vectorial transport of bile acids from the portal blood into the hepatocytes via NTCP and then into the intrahepatic biliary system via BSEP (bile salt export pump). BSEP is a member of the ABC (ATP-binding-cassette) transporter family and is classified as ABCB11 (ABC subfamily B, member 11). BSEP is regulated both transcriptionally and post-translationally, and mediates canalicular bile formation [17]. In the present study, we show that hepatic LKB1 plays a key role in liver cellular architecture and metabolism. Absence of hepatic LKB1 results in mis-localization of BSEP, bile duct paucity and impairment of postnatal biliary tree formation. LLKB1KO (liver-specific *Lkb1*-knockout) mice also display impaired bile acid and lipid metabolism, and die within 4 weeks of birth.

MATERIALS AND METHODS

Generation of mice lacking hepatic LKB1

Production of mice harbouring *Lkb1*-floxed alleles has been described previously [14]. These mice were crossed with *B6.Cg-Tg* (*Alb-Cre*) *21 Mgn/J* transgenic mice harbouring *Cre*-recombinase under the albumin promoter (Jackson Laboratories). All animal studies were performed in accordance with the Animal Scientific Procedures Act. Animals were killed by cervical dislocation, and organs were rapidly removed and frozen in liquid nitrogen.

Western blotting

Proteins were resolved on 4–12 % gradient gels (Novex, Invitrogen), transferred on to PVDF membranes and probed with antibodies as described in the text. Antibodies were detected by ECL (enhanced chemiluminescence) (West Dura kit; Pierce).

Antibodies

The sheep anti-LKB1 antibody, raised against residues 24–39 of human LKB1, was generously provided by Professor Dario Alessi (Division of Signal Transduction Therapy, University of Dundee, Dundee, Scotland, U.K.). The mouse monoclonal anti-LKB1 antibody (Ley37D/G6) and goat anti-radixin antibody were from Santa Cruz Biotechnology. Rabbit anti-LKB1 antiserum [18], rabbit pan-AMPKβ antibody and sheep anti-AMPKα1 and -AMPKα2 antibodies [19] were as described previously. The anti-BSEP and -NTCP antibodies were generously provided by Professor Bruno Stieger (Division of Clinical Pharmacology and Toxicology, University Hospital, Zurich, Switzerland) [20,21]. The goat anti-(mouse osteopontin) antibody was from R&D Systems, and the anti-CK19 antibody was from Dako (IS615).

Haemocrit measurement

Blood was collected in haemocrit tubes and centrifuged at 3000 ***g***. Packed red cell volume was measured as a ratio of the total blood sample volume.

Immune complex kinase assays

LKB1 or AMPK complexes were immunoprecipitated from soluble liver lysates using antibodies bound to either Protein A– or Protein G–Sepharose. After extensive washing, kinase activity present in the immune complexes was determined as described previously [3]. AMPK activity was measured by [^{32}P]P_i incorporation into the SAMS peptide (HMRSAMSGLHLVKRR) [22]. LKB1 activity was measured by activation of bacterially expressed AMPK complex (α1, β1 and γ1), which was subsequently assayed using the SAMS peptide.

Osmotic fragility test

The osmotic fragility test was performed according to the method described by Foller et al. [23].

Transmission electron microscopy

After glutaraldehyde fixation and processing, samples were embedded in araldite. Semi-thin sections of 0.5–1 μm were stained with Toluidine Blue in borax. Ultra-thin sections were stained in uranyl acetate followed by Reynold's lead citrate.

Histology and immunohistochemistry

Tissue was fixed in formalin/saline and processed in paraffin wax. Routine sections were stained with haematoxylin and eosin. Immunohistochemical staining was carried out on the Dako Autostainer Plus using a diaminobenzidine-based system to identify antibody binding.

Immunofluorescence microscopy

Livers were fixed in paraformaldehyde, and frozen sections were used for staining. Appropriate Alexa Fluor® 488-conjugated secondary antibodies were used, and DAPI (4′,6-diamidino-2-phenylindole) was used as a nuclear stain.

Liver function tests and metabolite measurements

Serum levels of albumin, ALP (alkaline phosphatase), total cholesterol, LDL (low-density lipoprotein)-cholesterol and HDL (high-density lipoprotein)-cholesterol, bilirubin and triacylglycerols (triglycerides) were determined by the Mouse Biochemistry Laboratories, Cambridge, U.K. Assays were measured colorimetrically on a Dade Behring RXL autoanalyser. Esterified and non-esterified cholesterol measurements were made using an Amplex Red Cholesterol kit (Molecular Probes). Bile acids were measured using a TBA bile acid kit (Sentinel Diagnostics). Bile acids were extracted from livers by homogenization ten times in 70 % (v/v) ethanol.

Isolation of hepatocytes

Hepatocytes were isolated by collagenase perfusion of livers from 14–18-day-old anaesthetized mice. After isolation, cells were seeded in collagen-coated dishes in Medium 199 with Earle's salts and L-glutamine (Gibco) supplemented with UltroserG (Pall Life Sciences), 1 % (w/v) albumin, 100 nM insulin, 100 nM T_3 (tri-iodothyronine) and 100 nM dexamethasone. After cell attachment, the hepatocytes were cultured for 16–18 h in the absence of T_3, albumin and UltroserG and in the presence of 1 nM insulin

Bile acid uptake assay

The bile acid uptake assay was carried out as described previously [24].

Table 1 Sequences of the oligonucleotide primers used for qRT-PCR

Srebp, sterol-regulatory-element-binding protein; *HmgCoAR*, 3-hydroxy-3-methylglutaryl-CoA reductase.

mRNA	Forward (5′→3′)	Reverse (5′→-3′)
Abcg5	TGGGTCCCAAGGAGTATGC	GCTCCAAGACTTCACACAGTG
Abcg8	AGTGGTCAGTCCAACACTCTG	GAGACCTCCAGGGTATCTTGAA
Bsep	GGGAGCAGTGGGTGTGGTAAAAG	TCCTGGGAGACAATCCCAATGTT
Cypb	TGGAGAGCACCAAGACAGACA	TGCCGGAGTCGACAATGAT
Cyp7a1	AGCAACTAAACAACCTGCCAGTACTA	GTCCGGATATTCAAGGATGCA
Fxr	GGCAGAATCTGGATTTGGAATCG	GCTGAACTTGAGGAAACGGG
HmgCoAR	GATTCTGGCAGTCAGTGGGAA	GTTGTAGCCGCCTATGCTCC
Mrp2	ATGAAGTGACAGAGGGCGGT	TGCAGCCTGTGTGCGATAG
Mrp3	GCAGCAGAACCAAGCATCAAG	GACCGCATCCTCACCTGG
Mrp4	GGTTGGAATTGTGGGCAGAA	TCGTCCGTGTGGTCATTGAA
Ntcp	CTGCCGCCTGGCTTTGGCCA	CTGGAGCAGGTGGTCATCAC
Oatp1	TGATACACGCTGGGTCGGTG	GCTGCTCCAGGTATTTGGGC
Shp	CGATCCTCTTCAACCCAGATG	AGGGCTCCAAGACTTCACACA
Srebp1a	GTTGATGAGCTGGAGCATGT	CTCCCTCCTTACCCTTGGAG
Srebp1c	GGAGCCATGGATTGCACATT	GCTTCCAGAGAGGAGGCCAG
Srebp2	GCGTTCTGGAGACCATGGA	ACAAAGTTGCTCTGAAAACAAATCA

qRT (quantitative real-time)-PCR analysis

RNA was isolated from livers by homogenization in TRIzol® reagent (Invitrogen), according to the manufacturer's instructions, followed by purification on an RNeasy column (Qiagen). A total of 2 μg of RNA was used for first-strand cDNA synthesis using Superscript II (Invitrogen), according to the manufacturer's instructions, and qRT-PCR was performed with SensiMix Plus SYBR kit (Quantace) using Opticon DNA Engine. All primers used are shown in Table 1. All values are shown relative to the expression of *Cypb* (cyclophilin b).

Hepatic glucose output measurement

At 16 h after isolation, hepatocytes were transferred into glucose-free DMEM (Dulbecco's modified Eagle's medium) (Sigma) containing 2 mM sodium pyruvate and 20 mM lactate. Aliquots of medium were removed for glucose measurement at the stated times using a glucose oxidase kit (Thermo Scientific), according to the manufacturer's instructions.

Statistical analysis

All results are presented as means$\pm$S.E.M. In order to determine statistical significance, an unpaired two-tailed Student's *t* test was performed for the analysis of two groups, whereas data involving more than two groups were assessed using ANOVA. Statistically significant differences from wild-type were considered for *P* values <0.05.

RESULTS

Generation of LLKB1KO mice

We crossed mice expressing *Cre*-recombinase under the control of the albumin promoter [25] with mice harbouring floxed alleles of *Lkb1* [14] to generate $Cre^{+/-}Lkb1^{fl/fl}$ animals lacking LKB1 expression in the liver. PCR for the recombination event in a range of tissues demonstrated deletion of *Lkb1* specifically in the liver (Figure 1A). LKB1 protein expression was not detectable in liver extracts from 15-day-old LLKB1KO mice (Figure 1B). Hepatic LKB1 activity was barely detectable following birth and reached minimal levels by postnatal day 15 (Figure 1C), confirming functional deletion of LKB1 by 15 days of age. LKB1 protein expression and activity were also reduced in livers from $Lkb1^{fl/fl}$ mice (Figures 1B and 1C). These findings are consistent with a previous study [14] and arise due to the nature of the targeting event leading to a hypomorphic effect in several tissues. AMPK activity assayed in immune complexes isolated from liver extracts from LLKB1KO mice was drastically reduced relative to wild-type activity (Figure 1D). At 15 days, the activity of AMPKα1-containing complexes was reduced by approx. 90 % and AMPKα2 activity by >95 % in liver from LLKB1KO mice compared with the activity in liver extracts from wild-type mice (Figure 1D). There was also a slight reduction in AMPK activity in liver extracts isolated from $Lkb1^{fl/fl}$ mice, although this did not reach statistical significance for AMPKα2 complexes (Figure 1D). In previous studies, it was reported that deletion of LKB1 in skeletal muscle [26] or heart [27] resulted in loss of AMPKα2 activity, but AMPKα1 activity was only partially reduced or was up-regulated. Given the results obtained in the present study in liver, the contribution of LKB1 to activation of AMPKα1 appears to vary depending on the tissue type. LLKB1KO mice were noticeably smaller than either $Lkb1^{fl/fl}$ or wild-type mice and had significantly lower body weight from 4 days of age, and rapidly began to lose weight from around 15 days of age (Figure 1E). In contrast, the weight of livers isolated from LLKB1KO mice aged 15 days was significantly increased compared with wild-type mice (0.39 ± 0.045 g compared with 0.28 ± 0.008 g respectively, $n = 9$). This hepatomegaly resulted in a significant increase in the liver/body weight ratio (Figure 1F). By 12 days of age, LLKB1KO mice started to die and no LLKB1KO mice survived beyond 30 days of age (results not shown). We have been unable to find any obvious metabolic or growth phenotype for $Lkb1^{fl/fl}$, even though there is a significant decrease in LKB1 activity in a number of tissues in these mice compared with wild-type animals. One notable exception is that the male $Lkb1^{fl/fl}$ mice are infertile due to a defect in spermatogenesis, which has been described in a previous study [28].

LKB1 deletion leads to disrupted canalicular membranes and defective bile duct formation

In order to explore the increased mortality of the LLKB1KO mice, we undertook histological examination of the liver. No gross morphological changes were apparent and the LLKB1KO mouse had a patent common bile duct. In livers from LLKB1KO mice as young as 4 days old, there were increased bile ductular profiles, but no well-formed ducts around the portal tracts. This observation became more apparent with increasing age, as shown in Figure 2(A) for liver isolated from a 15-day-old animal. Identification of normal bile ducts was difficult in tissue from LLKB1KO mice 15 days old or older, whereas bile ducts were clearly visible in livers from wild-type animals at an equivalent age (Figures 2A–2C). Immunostaining for either osteopontin (Figure 2B), a protein excreted by biliary epithelial cells, or CK19 (Figure 2C), a biliary cytokeratin, showed staining in morphologically normal bile ducts in wild-type liver (indicated by * in Figure 2). Although there was staining in liver from LLKB1KO mice, this was associated with the increased bile ductular profiles (indicated by an arrow in Figure 2) and confirmed the lack of morphologically normal bile ducts. The expression of radixin, a protein usually located at hepatic canalicular membranes, was clearly reduced in livers from LLKB1KO mice (Figure 2D). In contrast, vascular staining in LLKB1KO mice appeared normal (indicated by 'v' in Figure 2, and results

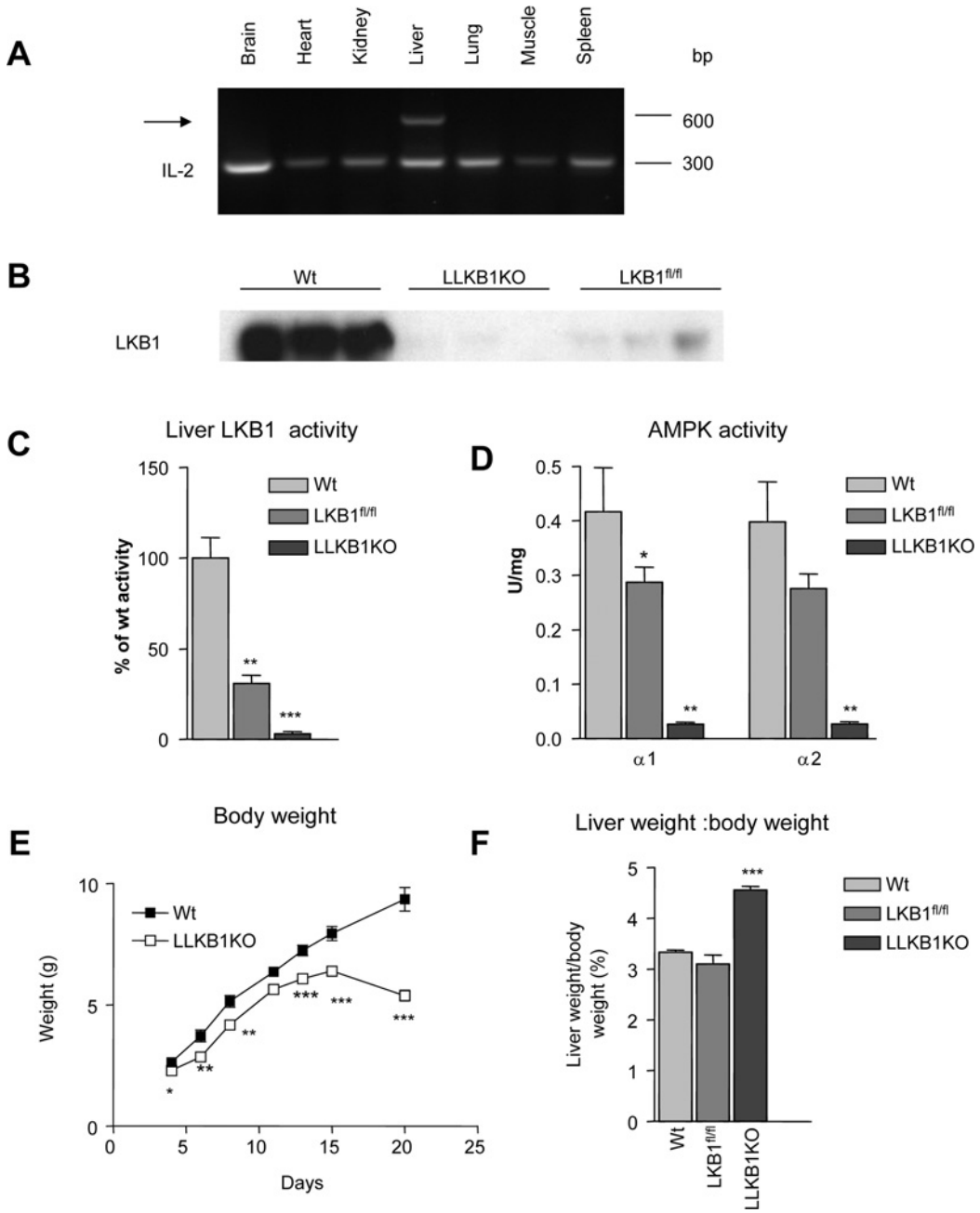

Figure 1 Liver-specific deletion of *Lkb1*

(**A**) DNA from tissues of 15-day-old mice and recombination of the floxed *Lkb1* allele detected by PCR. The recombination product is indicated by an arrow. IL-2 (interleukin-2) was used as an internal control. (**B**) LKB1 immune complexes from liver homogenates were immunoblotted for LKB1 in wild-type (Wt), $Lkb^{fl/fl}$ and LLKB1KO mice. (**C**) LKB1 activity measured in duplicate immune complexes from liver homogenates ($n = 3$). (**D**) AMPK activity was measured in AMPKα1- or α2-specific immune complexes isolated from liver homogenates of 15-day-old mice ($n = 5$). Results are expressed as units/mg of total protein, where 1 unit = 1 nmol of $^{32}PO_4$ incorporated into the SAMS peptide/min. (**E**) Body weights of wild-type or LLKB1KO mice are shown at the indicated days after birth ($n = 9$–11). (**F**). Liver weight/body weight ratio. Results are means$\pm$S.E.M. Statistically significant differences from wild-type are shown by * ($P < 0.05$), ** ($P < 0.01$) and *** ($P < 0.001$).

not shown). Transmission electron microscopy revealed ordered open canalicular channels (c) with well-defined microvilli (mv) in sections of livers from wild-type mice (Figure 3A). In livers from LLKB1KO mice, abnormal canaliculi were apparent with microvilli often appearing 'glued' together from as young as 6 days old. An example of a liver from a 15-day-old mouse is shown in Figure 3(B). In order to determine liver function, serum levels of several liver markers were measured. By 15 days of age, serum levels of ALP, ALT (alanine transaminase) and AST (aspartate transaminase) were all significantly increased in LLKB1KO mice (Figure 3C), whereas albumin levels were lower compared with wild-type (Figure 3D). By 15–20 days, there were patchy areas of necrosis within livers from LLKB1KO mice (Figure 3E). No significant differences were detected in $Lkb1^{fl/fl}$

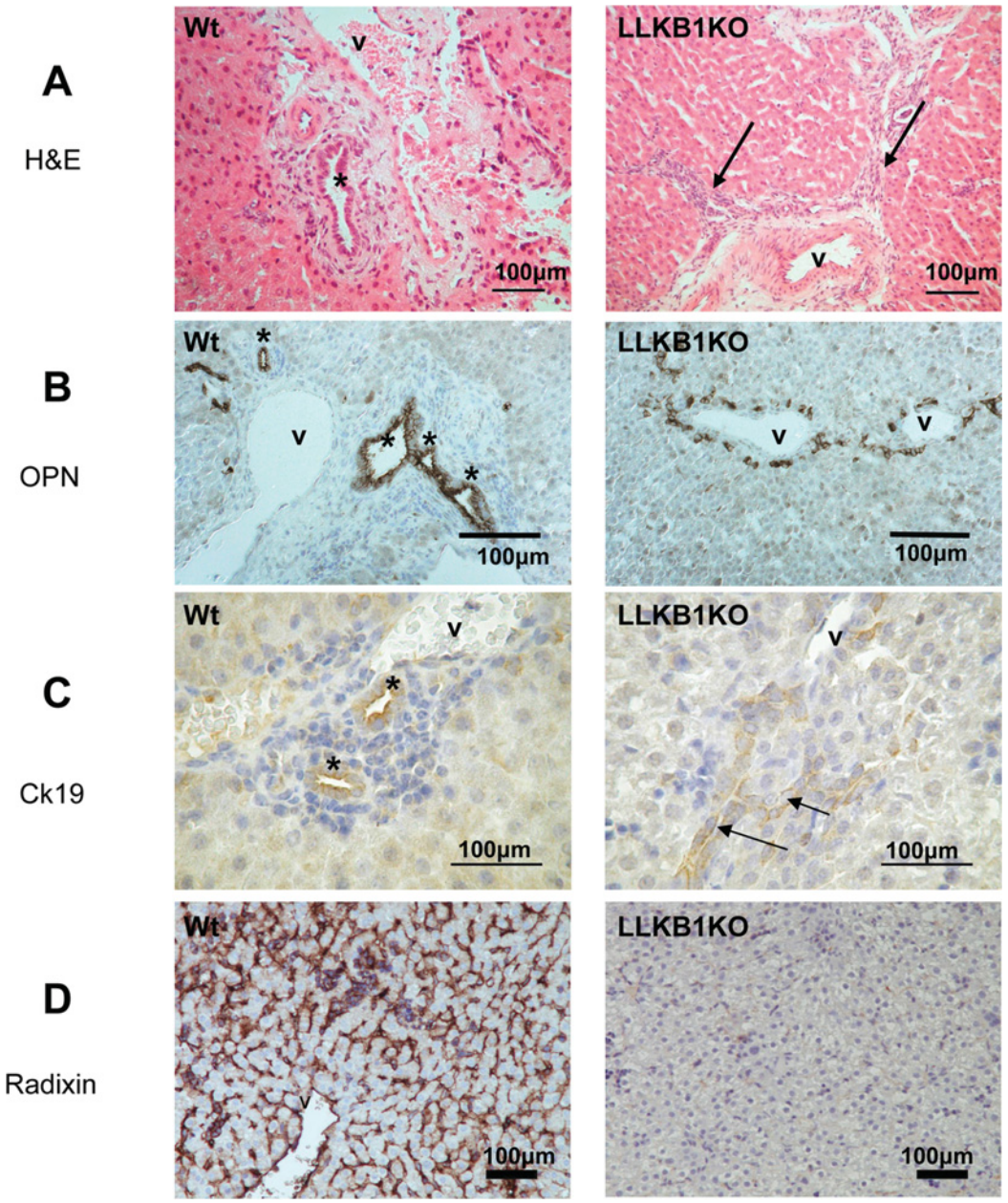

Figure 2 Altered liver architecture in livers from LLKB1KO mice

Livers from 15-day-old wild-type (Wt) and LLKB1KO mice were stained with haematoxylin and eosin (H&E) (**A**), and immunostained with osteopontin (OPN) (**B**), CK19 (**C**) or radixin (**D**). Arrows indicate increased bile ductular profiles and no morphologically normal open bile ducts in LLKB1KO mice. Normal bile ducts are indicated with * and blood vessels are labelled 'v' in each case. An example representative of at least three livers is shown.

mice compared with wild-type mice (Figure 3, and results not shown).

LLKB1KO mice display marked changes in cholesterol and bile acid metabolism

Given the abnormal liver architecture and in particular the lack of normal bile ductule formation in the LLKB1KO mice, we investigated cholesterol and bile acid metabolism in these animals. Serum cholesterol levels were significantly elevated in LLKB1KO mice by 8 days of age and continued to rise with increasing age (Figure 4A). In wild-type mice, only 15 % of circulating cholesterol was non-esterified, whereas in LLKB1KO mice more than 50 % was non-esterified (Figure 4B). Measured at 15 days of age, total cholesterol was significantly higher and LDL-cholesterol was 10-fold higher in LLKB1KO mice compared with wild-type or *Lkb1*$^{fl/fl}$ mice, whereas HDL-cholesterol and triacyglycerol levels were not significantly changed (Figure 4C). There was a significant increase in the concentration of serum bile acids by 4 days of age in LLKB1KO mice relative to wild-type mice (Figure 4D). The increase in serum bile acids preceded the elevation in cholesterol levels (compare Figures 4A and 4D). Levels of bile acids in the livers of LLKB1KO mice were very high compared with wild-type, albeit with widely varying levels detected in individual mice (Figure 4E). The rate of

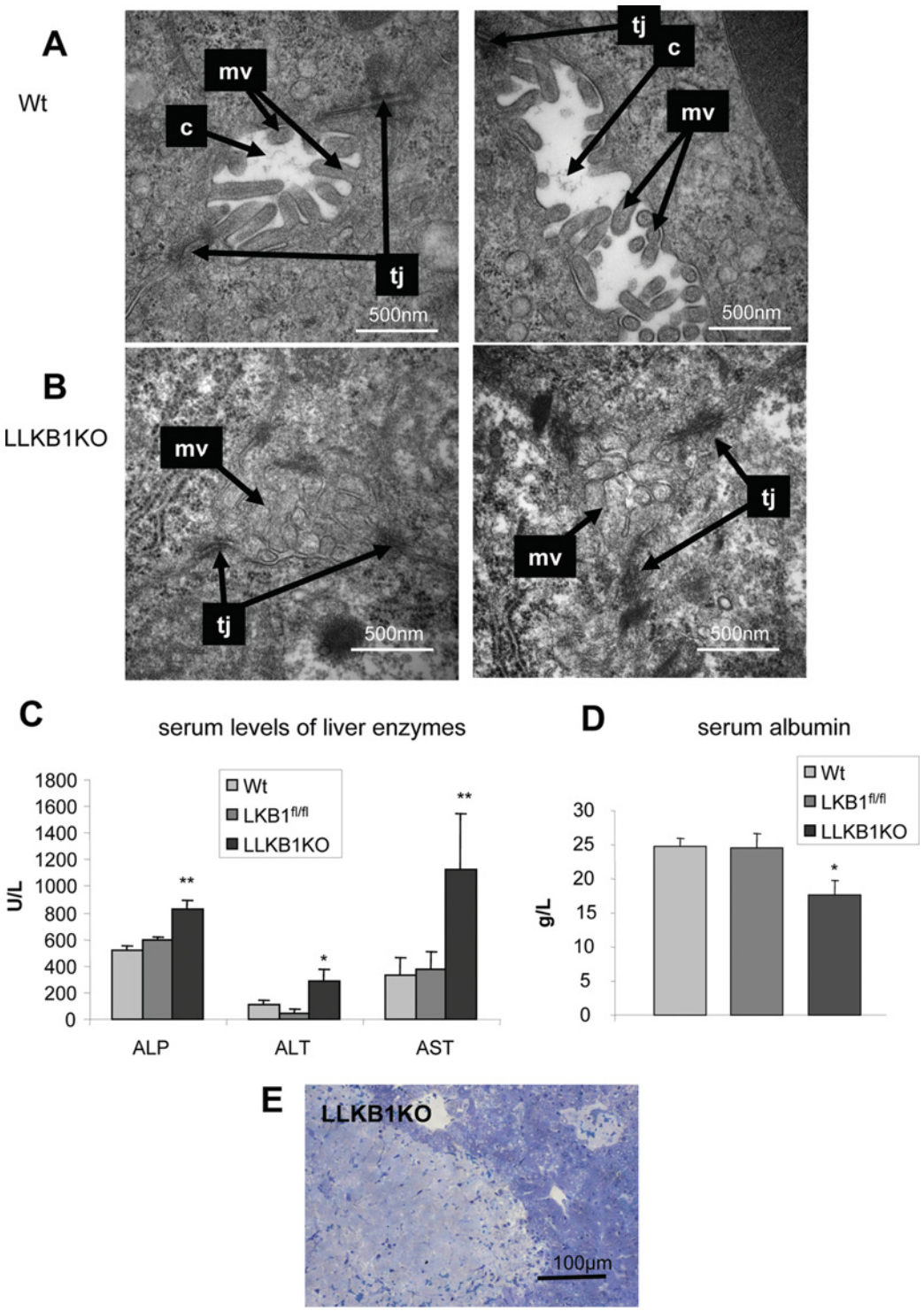

Figure 3 Altered canalicular morphology and liver function in LLKB1KO mice

Transmission electron micrographs of livers from 15-day-old wild-type (Wt) (**A**) and LLKB1KO (**B**) mice showing the canalicular membranes. The canalicular channel is labelled 'c', microvilli are labelled 'mv' and tight junctions are labelled 'tj'. A representative example of at least three livers is shown. (**C**) Serum levels of ALP, ALT and AST, and (**D**) albumin from 15-day-old wild-type (Wt) and LLKB1KO mice. Results are means$\pm$S.E.M. from $n = 5$ mice per genotype. Statistically significant differences from wild-type values are shown by * ($P < 0.05$) and ** ($P < 0.01$). (**E**) Toluene Blue-stained liver section from an 18-day-old LLKB1KO mouse showing 'patchy' necrosis. This is a representative image of three livers examined.

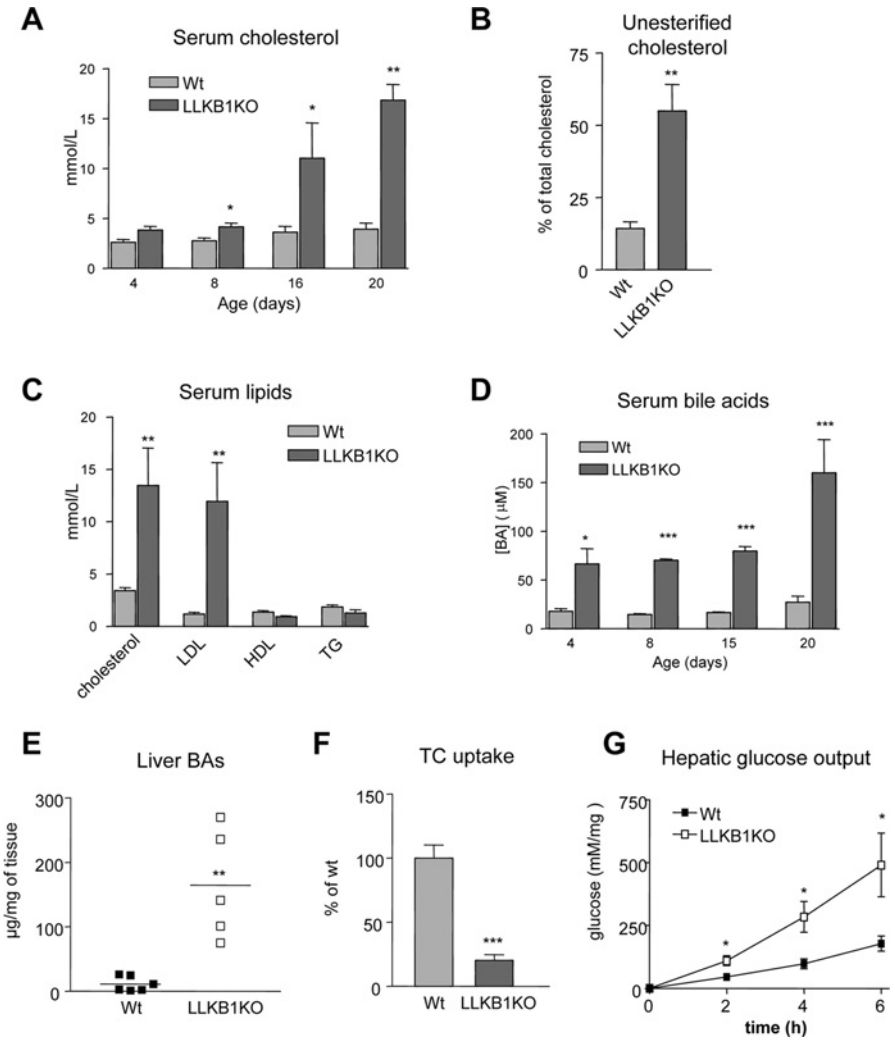

Figure 4 Lack of hepatic LKB1 disrupts cholesterol and bile acid metabolism

(**A**) Total serum cholesterol over time (age shown in days) ($n = 4$–6). (**B**) Non-esterified (unesterified) cholesterol as a percentage of total serum cholesterol in 15-day-old mice ($n = 4$–6). (**C**) Total cholesterol, LDL-cholesterol, HDL-cholesterol and triacylglycerol (TG) concentrations from serum of 15-day-old mice are shown ($n = 7$–10). (**D**) Serum bile acid concentrations ([BA]) over time (age in days) ($n = 4$–6). (**E**) Bile acids measured in liver extracts from wild-type (Wt) and LLKB1KO mice with the mean value shown by a bar ($n = 5$–6). (**F**) [^{3}H]Taurocholate (TC) uptake was measured in hepatocytes isolated from 15-day-old wild-type or LLKB1KO mice. Uptake is shown relative to wild-type cells. Triplicate measurements of three independent experiments are shown. In each case, results are means±S.E.M. Statistically significant differences from wild-type are indicated by * ($P < 0.05$), ** ($P < 0.01$) and *** ($P < 0.001$).

[^{3}H]taurocholate uptake in isolated hepatocytes from LLKB1KO mice was 5-fold lower than in wild-type cells (Figure 4F), which could contribute to the elevated levels of serum bile acids. In order to confirm that the hepatocytes isolated from the LLKB1KO animals are viable, we measured glucose output in these cells. Hepatic glucose output was increased in the LLKB1KO cells compared with wild-type cells under basal conditions (Figure 4G). This result is consistent with a previous study in which LKB1 was deleted in adult hepatocytes [29], and demonstrates that the hepatocytes isolated from LLKB1KO mice are metabolically competent to undergo gluconeogenesis, confirming their viability.

We went on to measure the expression of a number of genes known to play a role in bile acid transport and homoeostasis (Figure 5A). There was a significant change in some of the genes normally regulated by elevated levels of bile acids. The genes encoding the basolateral transporters OATP1 (organic anion transporting polypeptide 1) and NTCP were down-regulated, whereas expression of the gene encoding the basolateral efflux transporter MRP4 (multi-drug resistance protein 4) was increased. However, some of the genes expected to be altered by FXR activation due to high levels of bile acids, such as genes encoding SHP (small heterodimer partner), CYP7A1 (cytochrome P450, family 7, subfamily A, polypeptide 1), ABCG5/8 (ABC subfamily G, member 5/8), MRP3 and BSEP, were not significantly altered. In addition, we found a decrease in the expression of the gene encoding MRP2, which encodes a canalicular anion transporter, whereas other studies have found an increase in expression in response to elevated bile acids [16]. Despite the increase in cholesterol levels in the LLKB1KO mice, there were no significant changes in the expression of a number of genes involved in cholesterol biosynthesis (Figure 5B), suggesting that there is no overall up-regulation in cholesterol synthesis. Taken together, these findings led us to investigate whether the underlying cause of hepatic bile acid accumulation is a defect in bile acid clearance. This would be consistent with the lack of open bile ductules revealed by our histological analyses (Figure 2).

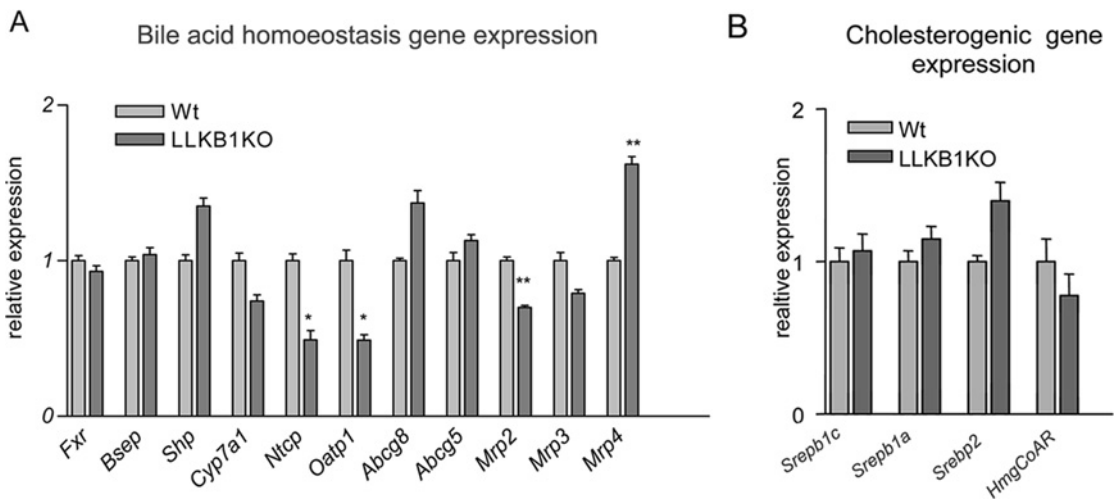

Figure 5 Expression of genes involved in bile acid and cholesterol homoeostasis

Expression levels of genes in livers of 15-day-old wild-type (Wt) or LLKB1KO mice measured by qRT-PCR for genes involved in bile acid homoeostasis (**A**) or cholesterol synthesis (**B**). The results are shown as relative expression normalized to *Cypb*, and the ratio of expression in livers from LLKB1KO mice is shown compared with wild-type (Wt) values set as 1 ($n = 6$). Results are means±S.E.M. Statistically significant differences from wild-type are indicated by * ($P < 0.05$) and ** ($P < 0.01$). *Srebp*, sterol-regulatory-element-binding protein; *HmgCoAR*, 3-hydroxy-3-methylglutaryl-CoA reductase.

Defective targeting of BSEP in LLKB1KO mice

Since our present findings indicate that increased bile acids in LLKB1KO mice result from defective clearance, we examined the expression of BSEP, one of the key components of bile acid efflux in the liver. BSEP protein expression was unchanged in livers from LLKB1KO mice, as measured by Western blotting (results not shown). We therefore extended our analysis to determine the localization of BSEP protein. In wild-type mice, as expected, BSEP was localized predominantly at the canalicular membrane (Figure 6A). In marked contrast, in liver from LLKB1KO mice, BSEP was found mainly within the cytoplasm, appearing to be associated with cytoplasmic vesicles (Figures 6A and 6B). There was no obvious difference in localization of NTCP, a basolateral membrane protein (Figure 6C). However, we observed lower NTCP staining in sections of liver from LLKB1KO mice compared with wild-type mice.

Loss of hepatic LKB1 leads to abnormal red blood cells and hyperbilirubinaemia

Examination of red blood cells from LLKB1KO mice at 18 days of age showed an abnormal morphology, exhibiting a 'spiky' appearance (Figure 7A). This altered morphology is similar to that described for spur cells of patients with severe liver disease [30]. The red blood cells from LLKB1KO mice were also shown to be more resistant to changes in osmolarity (Figure 7B). The packed red blood cell volume of LLKB1KO mice was significantly lower than that in wild-type mice (Figure 7C), implying that the LLKB1KO mice could be anaemic. Circulating levels of bilirubin, a product of heam breakdown, were dramatically increased in LLKB1KO mice, leading to a bright yellow coloration of the serum (Figure 7D). Bilirubin in serum from either wild-type or $Lkb1^{fl/fl}$ mice was virtually undetectable, whereas in LLKB1KO mice the levels were hugely elevated, the majority of which was conjugated which shows some functionality of the liver in the older mice.

DISCUSSION

In the present study, we have shown that mice lacking the expression of LKB1 in the liver have profound abnormalities in liver architecture and cell morphology that result in severe defects in bile and cholesterol metabolism. Although LKB1 activity was reduced in the liver of $Lkb1^{fl/fl}$ mice, there was no hepatic phenotype, suggesting that there is significant 'spare capacity' within the signalling pathway, and that LKB1 is not rate-limiting. This may be a more general feature of protein kinase signalling pathways, for example mice expressing 10 % of the normal levels of PDK1 (phosphoinositide-dependent kinase 1) appear normal, whereas complete deletion results in embryonic lethality [31]. Our present results show that LKB1 is required for the normal postnatal development of the biliary system, including correct localization of canalicular membrane proteins and development of bile ducts. The molecular mechanisms underlying development of the biliary tree are poorly understood. A number of other studies have demonstrated that LKB1 plays a key role in determining polarity in mammalian cells, as well as in other model organisms [32]. Activation of LKB1 has been shown to cause complete polarization of single mammalian epithelial cells [33]. An attractive hypothesis is that LKB1 is required for polarization of hepatocytes and that disruption of the normal development of the bile canaliculi in the LLKB1KO mice is a consequence of a defect in polarity determination. In support of this, we found that BSEP and radixin were no longer targeted to the canalicular membrane in the absence of LKB1. The failure to thrive and loss of weight of LLKB1KO mice may be caused by poor absorption of nutrients from the intestine due to the inability to transport bile from the liver via the biliary tree, which is defective in these animals.

Associated with the marked anatomical abnormalities observed in LLKB1KO mice we found a number of metabolic defects. There was a dramatic increase in serum and liver bile acids which stems from defective clearance of bile acids into the canaliculus as a direct consequence of mis-localization of BSEP. Previous studies have shown that bile acids regulate the transcription of

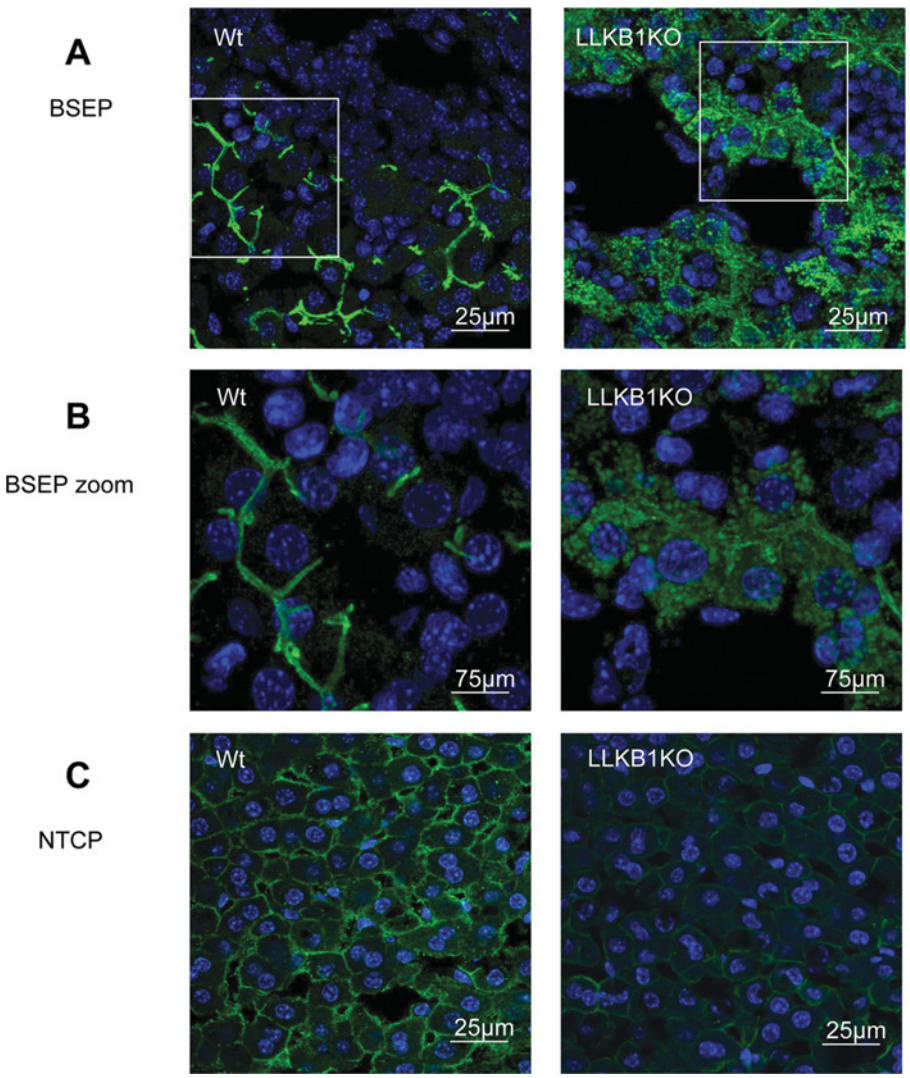

Figure 6 Cytoplasmic localization of BSEP in LLKB1KO livers

(**A**) Immunofluorescence staining for BSEP in 15-day-old mice with (**B**) magnification of the indicated areas shown in (**A**). (**C**) Immunostaining of NTCP in livers from 15-day-old mice. An example representative of at least three livers is shown.

genes encoding proteins involved in bile acid metabolism and transport. However, in spite of elevated circulating bile acids, some of the genes known to be transcriptionally controlled by FXR [34] were not altered in liver from LLKB1KO mice. We observed a decrease in the expression of the basolateral transporters *Oatp1* and *Ntcp*, as well as decreased staining of NTCP in the livers from LLKB1KO mice, which would explain a decrease in the taurocholate uptake in the isolated hepatocytes from LLKB1KO animals (Figure 4F). However, the expected transcriptional up-regulation of those transporters in the canalicular membrane, for example *Bsep*, *Abcg5/8* and *Mrp2*, is not apparent in the livers from LLKB1KO mice. There appears to be a lack of control of those genes involved in expression of proteins located to the canalicular membrane. Expression of the gene encoding CYP7A1, the rate-limiting enzyme in bile acid synthesis, is not decreased in response to the elevated bile acids in the livers from LLKB1KO mice. The intestine, as well as the liver, plays a critical role in bile acid homoeostasis. It has been shown that, in response to bile acids in the intestine, FXR stimulates FGF15 (fibroblast growth factor 15) expression in the intestine which signals via FGFR4 (FGF receptor 4) to bring about down-regulation of CYP7A1 in the liver. [35]. However, this route of control is likely to be defective in the LLKB1KO mice because bile acids are not flowing into the bile for release into the intestine and so cannot activate intestinal FXR. In this case, transcriptional suppression of CYP7A1 by FGF15 signalling would not be expected to occur, which may explain the modest decrease in expression that we observe in liver from LLKB1KO mice.

Dramatically elevated levels of circulating non-esterified cholesterol were observed in the LLKB1KO mice, which is most likely to be a secondary effect resulting from the reduced clearance of bile acids. It has been reported that cholestasis results in the appearance of a specific form of lipoprotein, LP-X (lipoprotein-X), which has a high content of non-esterified cholesterol and unusual protein content [36,37]. It is likely that LP-X makes up a proportion of the elevated LDL observed in the LLKB1KO mice. An attractive hypothesis is that the increased circulating free cholesterol leads to the defect in red blood cells that we observed in the LLKB1KO mice.

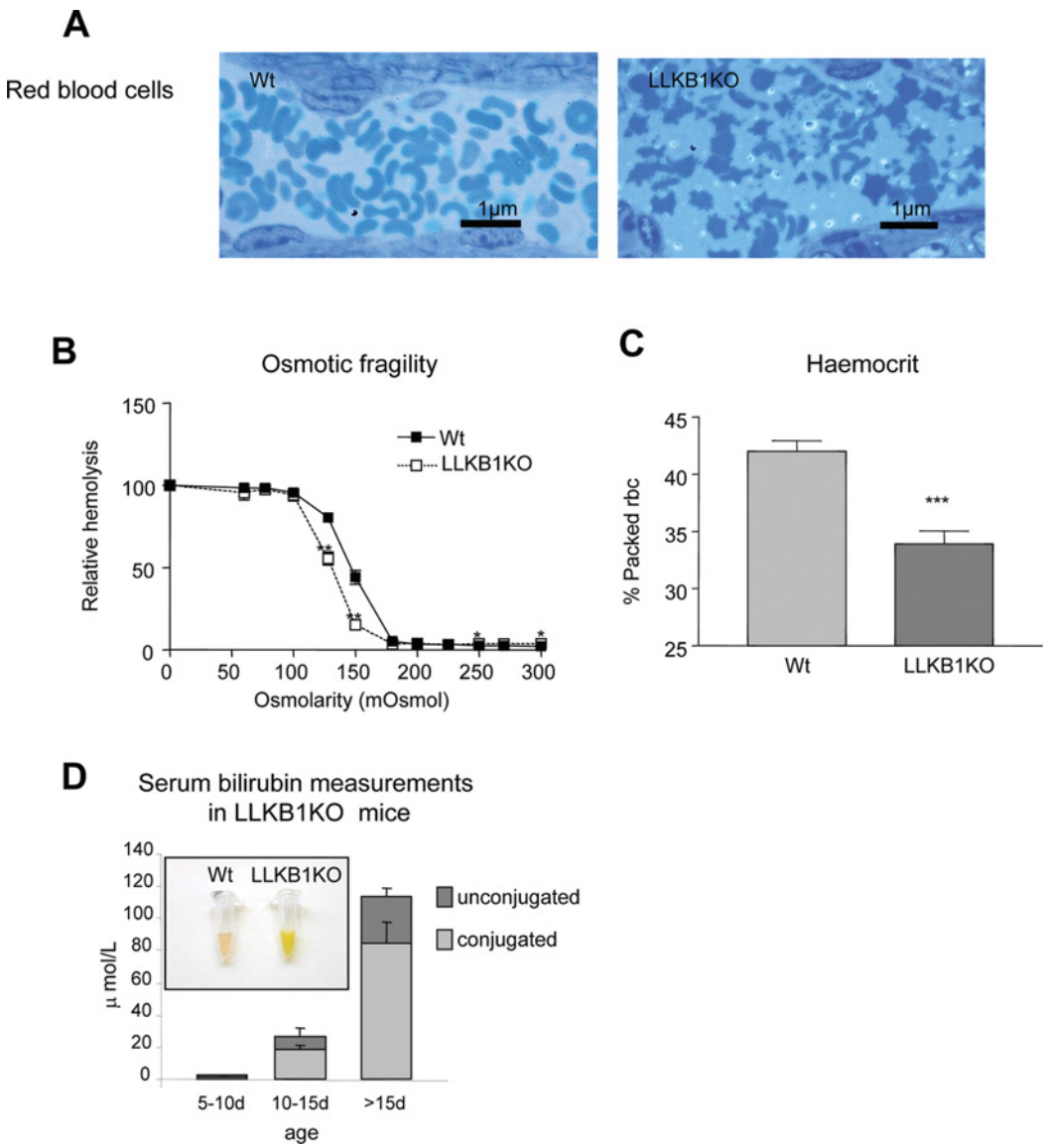

Figure 7 Development of hyperbilirubinaemia in LLKB1KO mice

(**A**) Semi-thin sections of livers from wild-type (Wt) or LLKB1KO mice showing red blood cells inside blood vessels of 18-day-old mice. An example representative of three livers of mice aged 18–21 days is shown. (**B**) Osmotic fragility of red blood cells isolated from 15-day-old wild-type and LLKB1KO mice. Relative haemolysis compared with 100 % in pure water (Os = 0) ($n = 6$). (**C**) Haemocrit values of 15-day-old mice ($n = 6$). rbc, red blood cell. (**D**) Serum levels of conjugated and unconjugated bilirubin from LLKB1KO mice of different ages (shown in days) ($n = 5$). Inset shows the marked yellow appearance of serum from LLKB1KO compared with wild-type mice. Results are means±S.E.M. Statistically significant differences from the wild-type values are shown by * ($P < 0.05$), ** ($P < 0.01$) and *** ($P < 0.001$).

Supporting this is a previous study that has shown that high circulating free cholesterol can alter the composition of the red blood cell membrane [38]. Excess membrane cholesterol leads to characteristic morphological abnormalities and formation of spur cells. The altered lipid composition of the red blood cell membrane results in spur cells with decreased deformability, which is essential for passage through capillary beds [39]. Destruction of the spur cells by the spleen ultimately leads to anaemia, as the bone marrow cannot produce sufficient new cells to compensate for the loss. The increased destruction of red blood cells leads to a further increase in circulating bilirubin, which cannot be appropriately disposed of in the bile due to defective canaliculi and bile ducts, thereby leading to excessive accumulation in the serum. It is apparent that the liver is able to conjugate the majority of the excess bilirubin, which shows the liver, even in late stages, maintains some functionality and the hyperbilirubinaemia is probably due to impaired transport and export from the liver. In a previous study, it has been shown that radixin deficiency causes conjugated hyperbilirubinaemia with loss of MRP2 (the major transporter of bilirubin) from the canalicular membranes [40]. As radixin is depleted in LLKB1KO mice, this is a possible explanation for elevated levels of conjugated bilirubin.

In a previous study in which LKB1 expression was deleted in adult liver [15], there was no report of altered bile acid or cholesterol metabolism. One possible reason for the absence of this phenotype could be that LKB1 activity was not completely abolished in that model, and that this might reduce the severity of the subsequent phenotype. However, an alternative explanation is that, in adult livers, biliary tree formation would have progressed

normally through development, precluding the onset of the phenotype we describe in our model.

The lack of open tubular bile ducts and areas of necrosis in the postnatal livers observed in livers from LLKB1KO mice are akin to observations seen in murine models of Alagille syndrome which are due to alterations in Notch signalling [41,42]. As in Notch2 inactivation, loss of LKB1 activity results in defective intrahepatic bile duct development. However, to date, there has been no direct connection made between Notch and LKB1 signalling pathways, although further investigation may be warranted.

In summary, in the present study we have shown a key role for LKB1 in co-ordinating the localization of canalicular membrane proteins and canalicular formation. The lack of LKB1 leads to the inability of the liver to transport and dispose of constituents of bile, resulting in a toxic build up of circulating bile acids, bilirubin and non-esterified cholesterol. It is noteworthy that deletion of both AMPKα1 and α2 in the liver does not result in a similar phenotype to the present model [43], but a very recent study in isolated hepatocytes reported a role for LKB1 and AMPK in the formation and maintenance of the canalicular network [44]. This finding supports a role for LKB1, AMPK and AMPK-related kinases in bile acid metabolism and canalicular formation. Further studies aimed at investigating the role of AMPK and the AMPK-related kinases downstream of LKB1 in hepatic development and liver disease is warranted. In summary, our present study uncovers a new role for LKB1 in the liver adding to the list of diverse functions of this master regulatory kinase.

AUTHOR CONTRIBUTION

Angela Woods designed and carried out the biochemical experiments, assays and immunofluorescence studies as well as writing the manuscript. Amanda Heslegrave carried out the biochemical experiments and assays. Phillip Muckett and Melanie Clements managed the animal experiments. Adam Levene and Robert Goldin were responsible for the histology and immunohistochemistry. Margaret Mobberely and Timothy Ryder performed the electron microscopy. Shadi Abu-Hayyeh performed the hepatic bile acid uptake assay. Alan Ashworth generated the LKB1 floxed transgenic mice. Catherine Williamson and Dominic Withers helped with the interpretation of the data. David Carling managed the project, and helped with the interpretation of the data, scientific discussion and writing the manuscript.

ACKNOWLEDGEMENTS

We thank Hiromi Kudo (Imperial College, London, U.K.) for her technical assistance, Professor Bruno Steiger for the anti-BSEP and NTCP antibodies, and Professor Dario Alessi for the anti-LKB1 antibodies.

FUNDING

This work was supported by the Medical Research Council, U.K (to A.W. and D.C.). A.J.H. was funded by an Integrated Project of the European Commission (EXGENESIS) [grant number LSHM-CT-2004–005272].

REFERENCES

1 Hemminki, A., Markie, D., Tomlinson, I., Avizienyte, E., Roth, S., Loukola, A., Bignell, G., Warren, W., Aminoff, M., Hoglund, P. et al. (1998) A serine/threonine kinase gene defective in Peutz–Jeghers syndrome. Nature **391**, 184–187

2 Jenne, D. E., Reimann, H., Nezu, J. I., Friedel, W., Loff, S., Jeschke, R., Müller, O., Back, W. and Zimmer, M. (1998) Peutz–Jeghers syndrome is caused by mutations in a novel serine threonine kinase. Nat. Genet. **18**, 38–43

3 Woods, A., Johnstone, S. R., Dickerson, K., Leiper, F. C., Fryer, L. G., Neumann, D., Schlattner, U., Wallimann, T., Carlson, M. and Carling, D. (2003) LKB1 is the upstream kinase in the AMP-activated protein kinase cascade. Curr. Biol. **13**, 2004–2008

4 Hawley, S. A., Boudeau, J., Reid, J. L., Mustard, K. J., Udd, L., Makela, T. P., Alessi, D. R. and Hardie, D. G. (2003) Complexes between the LKB1 tumor suppressor, STRADα/β and MO25α/β are upstream kinases in the AMP-activated protein kinase cascade. J. Biol. **2**, 28

5 Shaw, R. J., Kosmatka, M., Bardeesy, N., Hurley, R. L., Witters, L. A., DePinho, R. A. and Cantley, L. C. (2004) The tumor suppressor LKB1 kinase directly activates AMP-activated kinase and regulates apoptosis in response to energy stress. Proc. Natl. Acad. Sci. U.S.A. **101**, 3329–3335

6 Lizcano, J. M., Goransson, O., Toth, R., Deak, M., Morrice, N. A., Boudeau, J., Hawley, S. A., Udd, L., Makela, T. P., Hardie, D. G. and Alessi, D. R. (2004) LKB1 is a master kinase that activates 13 kinases of the AMPK subfamily, including MARK/PAR-1. EMBO J. **23**, 833–843

7 Alessi, D. R., Sakamoto, K. and Bayascas, J. R. (2006) LKB1-dependent signaling pathways. Annu. Rev. Biochem. **75**, 137–163

8 Cohen, D., Brennwald, P. J., Rodriguez-Boulan, E. and Musch, A. (2004) Mammalian PAR-1 determines epithelial lumen polarity by organizing the microtubule cytoskeleton. J. Cell Biol. **164**, 717–727

9 Barnes, A. P., Lilley, B. N., Pan, Y. A., Plummer, L. J., Powell, A. W., Raines, A. N., Sanes, J. R. and Polleux, F. (2007) LKB1 and SAD kinases define a pathway required for the polarization of cortical neurons. Cell **129**, 549–563

10 Kishi, M., Pan, Y. A., Crump, J. G. and Sanes, J. R. (2005) Mammalian SAD kinases are required for neuronal polarization. Science **307**, 929–932

11 Bright, N. J., Thornton, C. and Carling, D. (2009) The regulation and function of mammalian AMPK-related kinases. Acta Physiol. **196**, 15–26

12 Ylikorkala, A., Rossi, D. J., Korsisaari, N., Luukko, K., Alitalo, K., Henkemeyer, M. and Makela, T. P. (2001) Vascular abnormalities and deregulation of VEGF in *Lkb1*-deficient mice. Science **293**, 1323–1326

13 Hezel, A. F., Gurumurthy, S., Granot, Z., Swisa, A., Chu, G. C., Bailey, G., Dor, Y., Bardeesy, N. and De Pinho, R. A. (2008) Pancreatic LKB1 deletion leads to acinar polarity defects and cystic neoplasms. Mol. Cell. Biol. **28**, 2414–2425

14 Sakamoto, K., McCarthy, A., Smith, D., Green, K. A., Grahame Hardie, D., Ashworth, A. and Alessi, D. R. (2005) Deficiency of LKB1 in skeletal muscle prevents AMPK activation and glucose uptake during contraction. EMBO J. **24**, 1810–1820

15 Shaw, R. J., Lamia, K. A., Vasquez, D., Koo, S. H., Bardeesy, N., Depinho, R. A., Montminy, M. and Cantley, L. C. (2005) The kinase LKB1 mediates glucose homeostasis in liver and therapeutic effects of metformin. Science **310**, 1642–1646

16 Lefebvre, P., Cariou, B., Lien, F., Kuipers, F. and Staels, B. (2009) Role of bile acids and bile acid receptors in metabolic regulation. Physiol. Rev. **89**, 147–191

17 Stieger, B., Meier, Y. and Meier, P. J. (2007) The bile salt export pump. Pflügers Arch. **453**, 611–620

18 Denison, F. C., Hiscock, N. J., Carling, D. and Woods, A. (2009) Characterization of an alternative splice variant of LKB1. J. Biol. Chem. **284**, 67–76

19 Woods, A., Cheung, P. C., Smith, F. C., Davison, M. D., Scott, J., Beri, R. K. and Carling, D. (1996) Characterization of AMP-activated protein kinase β and γ subunits. Assembly of the heterotrimeric complex *in vitro*. J. Biol. Chem. **271**, 10282–10290

20 Gerloff, T., Stieger, B., Hagenbuch, B., Madon, J., Landmann, L., Roth, J., Hofmann, A. F. and Meier, P. J. (1998) The sister of P-glycoprotein represents the canalicular bile salt export pump of mammalian liver. J. Biol. Chem. **273**, 10046–10050

21 Stieger, B., Hagenbuch, B., Landmann, L., Hochli, M., Schroeder, A. and Meier, P. J. (1994) In situ localization of the hepatocytic Na^+/taurocholate cotransporting polypeptide in rat liver. Gastroenterology **107**, 1781–1787

22 Davies, S. P., Carling, D. and Hardie, D. G. (1989) Tissue distribution of the AMP-activated protein kinase, and lack of activation by cyclic-AMP-dependent protein kinase, studied using a specific and sensitive peptide assay. Eur. J. Biochem. **186**, 123–128

23 Foller, M., Sopjani, M., Koka, S., Gu, S., Mahmud, H., Wang, K., Floride, E., Schleicher, E., Schulz, E., Munzel, T. and Lang, F. (2009) Regulation of erythrocyte survival by AMP-activated protein kinase. FASEB J. **23**, 1072–1080

24 Abu-Hayyeh, S., Martinez-Becerra, P., Sheikh Abdul Kadir, S. H., Kadir, A., Selden, C., Romero, M. R., Rees, M., Marschall, H.-U., Marin, J. J. G. and Williamson, C. (2010) Inhibition of Na^+-taurocholate co-transporting polypeptide mediated bile acid transport by cholestatic sulphated progesterone metabolites. J. Biol. Chem. **285**, 16504–16512

25 Postic, C., Shiota, M., Niswender, K. D., Jetton, T. L., Chen, Y., Moates, J. M., Shelton, K. D., Lindner, J., Cherrington, A. D. and Magnuson, M. A. (1999) Dual roles for glucokinase in glucose homeostasis as determined by liver and pancreatic β cell-specific gene knock-outs using Cre recombinase. J. Biol. Chem. **274**, 305–315

26 McGee, S. L., Mustard, K. J., Hardie, D. G. and Baar, K. (2008) Normal hypertrophy accompanied by phosphoryation and activation of AMP-activated protein kinase α1 following overload in LKB1 knockout mice. J. Physiol. **586**, 1731–1741

27 Sakamoto, K., Zarrinpashneh, E., Budas, G. R., Pouleur, A. C., Dutta, A., Prescott, A. R., Vanoverschelde, J. L., Ashworth, A., Jovanovic, A., Alessi, D. R. and Bertrand, L. (2006) Deficiency of LKB1 in heart prevents ischemia-mediated activation of AMPKα2 but not AMPKα1. Am. J. Physiol. Endocrinol. Metab. **290**, E780–E788

28 Towler, M. C., Fogarty, S., Hawley, S. A., Pan, D. A., Martin, D. M. A., Morrice, N. A., McCarthy, A., Galardo, M. N., Meroni, S. B., Cigorraga, S. B. et al. (2008) A novel short splice variant of the tumour suppressor LKB1 is required for spermiogenesis. Biochem. J. **416**, 1–14
29 Foretz, M., Hebrard, S., Leclerc, J., Zarrinpashneh, E., Soty, M., Mithieux, G., Sakamoto, K., Andreelli, F. and Viollet, B. (2010) Metformin inhibits hepatic gluconeogenesis in mice independently of the LKB1/AMPK pathway via a decrease in hepatic energy state. J. Clin. Invest. **120**, 2355–2369
30 Cooper, R. A. (1969) Anemia with spur cells: a red cell defect acquired in serum and modified in the circulation. J. Clin. Invest. **48**, 1820–1831
31 Lawlor, M. A., Mora, A., Ashby, P. R., Williams, M. R., Murray-Tait, V., Malone, L., Prescott, A. R., Lucocq, J. M. and Alessi, D. R. (2002) Essential role of PDK1 in regulating cell size and development in mice. EMBO J. **21**, 3728–3738
32 Baas, A. F., Smit, L. and Clevers, H. (2004) LKB1 tumor suppressor protein: PARtaker in cell polarity. Trends Cell Biol. **14**, 312–319
33 Baas, A. F., Kuipers, J., Van Der Wel, N. N., Batlle, E., Koerten, H. K., Peters, P. J. and Clevers, H. C. (2004) Complete polarization of single intestinal epithelial cells upon activation of LKB1 by STRAD. Cell **116**, 457–466
34 Eloranta, J. J. and Kullak-Ublick, G. A. (2005) Coordinate transcriptional regulation of bile acid homeostasis and drug metabolism. Arch. Biochem. Biophys. **433**, 397–412
35 Inagaki, T., Choi, M., Moschetta, A., Peng, L., Cummins, C. L., McDonald, J. G., Luo, G., Jones, S. A., Goodwin, B., Richardson, J. A. et al. (2005) Fibroblast growth factor 15 functions as an enterohepatic signal to regulate bile acid homeostasis. Cell Metab. **2**, 217–225
36 Walli, A. K. and Seidel, D. (1984) Role of lipoprotein-X in the pathogenesis of cholestatic hypercholesterolemiaUptake of lipoprotein-X and its effect on 3-hydroxy-3-methylglutaryl coenzyme A reductase and chylomicron remnant removal in human fibroblasts, lymphocytes, and in the rat. J. Clin. Invest. **74**, 867–879
37 Seidel, D., Alaupovic, P. and Furman, R. H. (1969) A lipoprotein characterizing obstructive jaundice. I. Method for quantitative separation and identification of lipoproteins in jaundiced subjects. J. Clin. Invest. **48**, 1211–1223
38 Balistreri, W. F., Leslie, M. H. and Cooper, R. A. (1981) Increased cholesterol and decreased fluidity of red cell membranes (spur cell anemia) in progressive intrahepatic cholestasis. Pediatrics **67**, 461–466
39 Cooper, R. A., Durocher, J. R. and Leslie, M. H. (1977) Decreased fluidity of red cell membrane lipids in abetalipoproteinemia. J. Clin. Invest. **60**, 115–121
40 Kikuchi, S., Hata, M., Fukumoto, K., Yamane, Y., Matsui, T., Tamura, A., Yonemura, S., Yamagishi, H., Keppler, D., Tsukita, S. and Tsukita, S. (2002) Radixin deficiency causes conjugated hyperbilirubinemia with loss of Mrp2 from bile canalicular membranes. Nat. Genet. **31**, 320–325
41 Geisler, F., Nagl, F., Mazur, P., Lee, M., Zimber-Strobl, U., Strobl, L., Radtke, F., Schmid, R. M. and Siveke, J. T. (2008) Liver-specific inactivation of *Notch2*, but not *Notch1*, compromises intrahepatic bile duct development in mice. Hepatology **48**, 607–616
42 Ryan, M. J., Bales, C., Nelson, A., Gonzalez, D. M., Underkoffler, L., Segalov, M., Wilson-Rawls, J., Cole, S. E., Moran, J. L., Russo, P. et al. (2008) Bile duct proliferation in Jag1/fringe heterozygous mice identifies candidate modifiers of the Alagille syndrome hepatic phenotype. Hepatology **48**, 1989–1997
43 Guigas, B., Bertrand, L., Taleux, N., Foretz, M., Wiernsperger, N., Vertommen, D., Andreelli, F., Viollet, B. and Hue, L. (2006) 5-Aminoimidazole-4-carboxamide-1-β-D-ribofuranoside and metformin inhibit hepatic glucose phosphorylation by an AMP-activated protein kinase independent effect on glucokinase translocation. Diabetes **55**, 865–874
44 Fu, D., Wakabayashi, Y., Ido, Y., Lippincott-Schwartz, J. and Arias, I. M. (2010) Regulation of bile canalicular network formation and maintenance by AMP-activated protein kinase and LKB1. J. Cell Sci. **123**, 3294–3302

Received 22 October 2010/18 November 2010; accepted 30 November 2010
Published as BJ Immediate Publication 30 November 2010, doi:10.1042/BJ20101721